Friction Riveting (FricRiveting) as a new joining technique in GFRP lightweight bridge construction

L. Blaga[1a, 2], S.T. Amancio-Filho[1a], J. F. dos Santos[1], R. Bancila[2]

[1]) Helmholtz-Zentrum Geesthacht, Centre for Materials and Coastal Research, Institute of Materials Research, Materials Mechanics, Solid State Joining Processes, [a] Advanced Polymer-Metal Hybrid Structures, Geesthacht (Germany)

[2]) Universitatea "Politehnica" din Timişoara, Faculty for Civil Engineering, Deptartment for Steel Construction and Material Mechanics, Timisoara (Romania)

Abstract: GFRP lightweight bridges can be an efficient solution for emergency bridges, which are of vital importance in humanitarian missions following natural disasters or accidents. One of the main problems in the construction with composite structural materials is the joining technology. This study demonstrates the feasibility of the innovative Friction Riveting joining technique on glass fiber reinforced composite / lightweight alloy overlap joints for structural engineering applications. A case study of a glass fiber reinforced polyetherimide emergency bridge with friction-riveted (titanium grade 2 rivets) profiles connected by aluminum shoes (Al 2198-T851). Friction-riveted bridge joints would benefit of advantages such as high strengths, short joining cycles and absence of complex surface preparation. Recorded temperature history during FricRiveting revealed peak temperatures of up to 600 ºC, offering an important insight on the formation of the joint (plasticizing of the metallic rivet and physical-chemical structural changes). Microstructural investigation showed the formation of the rivet anchoring zone (deformed rivet tip with increased diameter) without extensive thermal changes of the matrix and mechanical destruction of the fiber woven. Hybrid friction-riveted composite/titanium grade 2 /aluminum overlap joints were successfully produced and optimized via design of experiments, revealing lap shear strengths of up to about 200 MPa and final fracture through shear of the metallic rivet. Results were compared with bolted connections in similar configuration and testing conditions; Experimental investigation indicated that joints by FricRiveting have comparable mechanical behavior and strength as bolted joints. The load requirement of 25 m span truss girder GFRP bridge with the proposed friction-riveted connections was calculated by finite element, leading to a number of 162 necessary M5 rivets for the joints with maximum axial forces of 760 kN. This work has successfully demonstrated the potential of friction riveting on structural engineering applications.

Keywords: Composite materials; lightweight structures; joining of composites; FricRiveting; emergency bridges

1. Introduction

After proving their effectiveness during the last 50 years in the aerospace-, marine- and automotive industries, glass fiber reinforced polymer (GFRP) composites emerged in the last two decades as materials suitable for civil engineering applications as well. High fabrication costs, lack of experience and gaps in knowledge of material properties and structural behavior were justified reasons for which the construction sector was one of the most conservative regarding the introduction of GFRP as a new structural material. GFRP profiles can work together or even replace classical construction materials steel and concrete; in fact the main purpose is not to replace classical materials, but to be applied as an efficient alternative, where their properties could add value for the desired structural applications [1].

1.1. GFRP in bridge construction

The premiere for the world's first GFRP bridge is being disputed by the 12 m span Ginzi Highway bridge in Bulgaria (Figure 1) and the Miyun Bridge in Beijing, China, both built in 1982 [2, 3]. Today, a few hundreds of pedestrian and vehicular bridges contain GFRP in deck elements, beams, trusses, rebar / concrete reinforcement rods, cables, tendons, reinforcements and panels. An estimated number of around 300 bridges worldwide are built entirely using fiber reinforced plastics (all-FRP structures).

Figure 1 – Ginzi Highway GFRP- Bridge, Bulgaria

Compared to classical structural materials, GFRP can be advantageous in bridge construction through their high specific strength (strength-to-weight ratio), resistance to corrosion, temperature and chemicals; Furthermore GFRP bridge elements are easy to

produce, transport and install (reduced installation costs) while they require only minimal maintenance (reduced service-life costs).

1.2. Emergency bridges

The worldwide climate changes in the last decades, as well as the growth of potential natural and non-natural (human being-originated) threats, increased the need of bridge structures with adequate load bearing capacity. Emergency bridges must simple design and fast to erect, at low costs at the same time. In emergency situations (flooding, earthquakes, accidents, terrorist and war blasts, etc.) interrupted transport connections must be re-established as fast as possible for rescue and humanitarian missions. One of the hot topics in bridge constructions identified recently by the international welding and joining community in the white paper of the International Institute of Welding [1] is the design and realization of prefabricated components. Typical prefabricated bridges can be erected much faster than a cast-in-place structure, therefore are the optimal solution for emergency hazard cases [2, 4].

Currently, the most used standardized emergency bridges are the Bailey Bridge and the D-Bridge. The highly versatile Bailey Bridge, developed in the 1940s by the British Royal Army [5], is erected by manpower only; it consists of steel segments – the so-called “Bailey panels” – each weighting 300 kg and is still a widely used concept for temporary bridging [6, 7]. The D-Bridge, developed in the 1960s by steel giant Krupp together with the truck producer MAN, is a dismountable steel truss girder structure, consisting of triangular elements, with a load-bearing capacity of a 30 tonne truck and reaching a maximum span of 90 m [5].

Another hot topic for future developments in bridge construction is the development and use of corrosion resistant structural materials, such as polymer composites. The international welding community has identified the corrosion of steel bridges as a key-problem, due to the large inspections costs and repair procedures need to avoid bridge premature collapse due to loss of section [1]. The selection of GFRP in bridge elements allows bridges to cope with corrosion and mechanical resistance requirements, being able to be used in different environments including those ones under salt-spray influence (e.g. coastal regions). Moreover GFRP structural elements are highly adequate for transportation and assembly of prefabricate bridge parts due to their lower weight.

An innovative lightweight 30 m span GFRP-truss bridge for emergency situations has been proposed and developed at the Technical University in Aachen, Germany in 2004 [8]. The structure consisting of pultruded-GFRP profiles was subject of detailed research, especially regarding the selection of joining techniques. A hybrid metallic bolting/adhesive bonding approach was applied to connect profiles with the addition of a metallic shoe for reinforcing the joint area [8, 9]. Figure 2 presents the structural details of this GFRP-truss bridge, weighting a total of 16 tonnes and designed for the load of a 40 tonne truck (according to standard MLC40) [8, 10] :

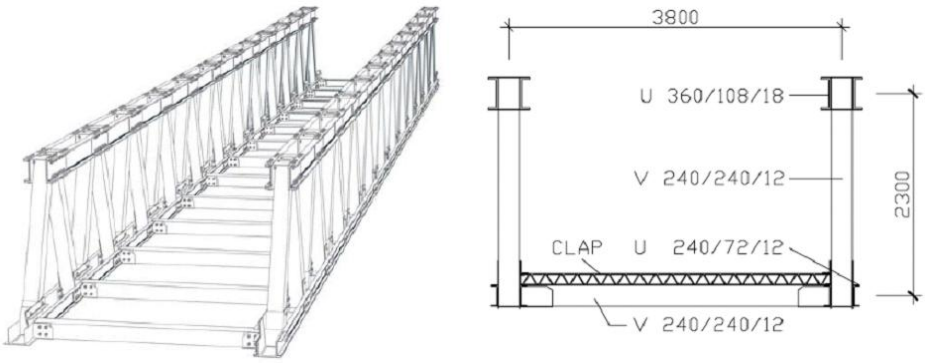

Figure 2 – Isometric and cross sectional views of the GFRP-lightweight-emergency-bridge [8]

1.3. State of the art in GFRP connections for structural profiles used in bridge construction

Joining of GFRP structural elements is one of the greatest challenges for civil and structural engineers. Joining technology for this new class of materials plays currently a central role in the research and development activities of the structural design community. *A priori* there are only three ways of joining materials and parts: by using and relying on mechanical and/or chemical forces, or by making use of and to depend on physical forces [11]. The available joining techniques for structural GFRP applications are adhesive bonding, mechanical fastening and hybrid bonded-bolted connections. Welding may also be an option, but only in the case of thermoplastic polymers and a few joint geometries [12].

Joining by adhesives, mostly one- or two-component epoxy-based, provides advantages such as lower stress concentration, good joint stiffness, low weight, minimal alteration of the chemical composition and microstructure of the adherends and the possibility

of joining dissimilar materials. The typical design implications and disadvantages related to adhesive bonding, which have to be taken into consideration and solved, are [13]:

- Non-uniform stress distribution in the adhesives
- Limited bond failure prediction and health monitoring of bonded structures
- Large sensitivity to temperature, chemical, ultraviolet radiation and moisture
- Bonded connections cannot be usually disassembled
- Need of complicated surface preparations: cleaning, solvent degreasing, pH neutralizing, abrasion (for epoxies)
- Longer curing times: two component epoxy-based adhesives require curing times of up to 24 hours in order to achieve the expected mechanical properties
- Adhesives can transfer only shear stresses
- Complex inspection and repair procedures

Bolted connections offer multiple advantages, such as disassembly ability, simple surface preparation, easy predictability of joint failure, simple inspection, easy handling and machining, fast assembly and joining times. But these advantages come at the expense of several disadvantageous issues in composite structures:

- Augmented stress concentrations due to the introduction of through-holes
- Reduction of the net cross sections
- Increased joint weight
- Torque limitations (variability in the bolt clamping force)
- Uneven load distribution to multiple rows of fasteners
- Creep and stress relaxation
- Temperature and moisture sensitivity

Hybrid bonding-and-bolting solutions can improve the joint stiffness, but do not necessarily increase its mechanical performance [14]. Mottram and Zheng [15] demonstrated in their work, that this increased joint stiffness leads to the decrease of the connection ductility and increases the susceptibility to brittle failure of the bonded-and-bolted joints.

Therefore there is an open niche to develop design-optimized, faster and cost-effective joining methodologies for polymer composite elements used in emergency bridge

construction. This work investigated for the first time the new friction riveting technology as an alternative, fast and simple joining technology to connect GRFP structural elements for future emergency bridge constructions. The feasibility of friction riveting was evaluated and optimized for different combination of GFRP/rivet/metallic shoe connector, through the use of design of experiments and statistical tools. After the accomplishment of joining procedure optimization, a case-study GFRP-emergency bridge design was selected to investigate the application of friction riveted GFRP truss girder elements; finite element modeling was used to determine load distribution in riveted node connections. Finally a fabrication procedure and design of friction riveted GFRP connections in truss-girder bridges were proposed based on available structural codes.

2. Friction Riveting

2.1. Principles of the technique

Friction Riveting, hence the name FricRiveting, is an innovative joining technique for polymer-metal hybrid structures, developed and patented by the Helmholtz Zentrum Geesthacht in Germany [16]. Joining is achieved by mechanical interference and adhesion between a metallic rivet and polymeric joining partners. The process is based on the principles of mechanical fastening and friction welding; the joining energy is supplied by the rotation of the metallic rivet, in form of frictional heat.

The process is primarily conceived to overlap joints, but can be better understood through the so called metallic-insert joint configuration (Figure 3). The process consists in rotating a cylindrical metallic rivet inserting it in a polymeric base plate fixed onto a backing plate. Heat is generated by the high rotational speed and the axial pressure. Due to the local increase of temperature, a molten polymeric layer is formed around the tip of the rotating rivet (Figure 3-B). By the end of the heating phase, the heat input rate increases to a higher level than the heat outflow, due to the low thermal conductivity of the polymer. The local temperature increases leading to the plasticizing of the tip of the rivet. While the rotation is decelerated, the axial pressure is concomitantly increased, the so-called forging pressure is applied and the plasticized tip of the rivet is being deformed (Figure 3C). As a result there will be an increase of the original rivet diameter, whereby the deformed rivet tip will assume a

parabolic pattern due to the opposite reactive forces related to the colder polymeric volumes (Figure 3D) [17].

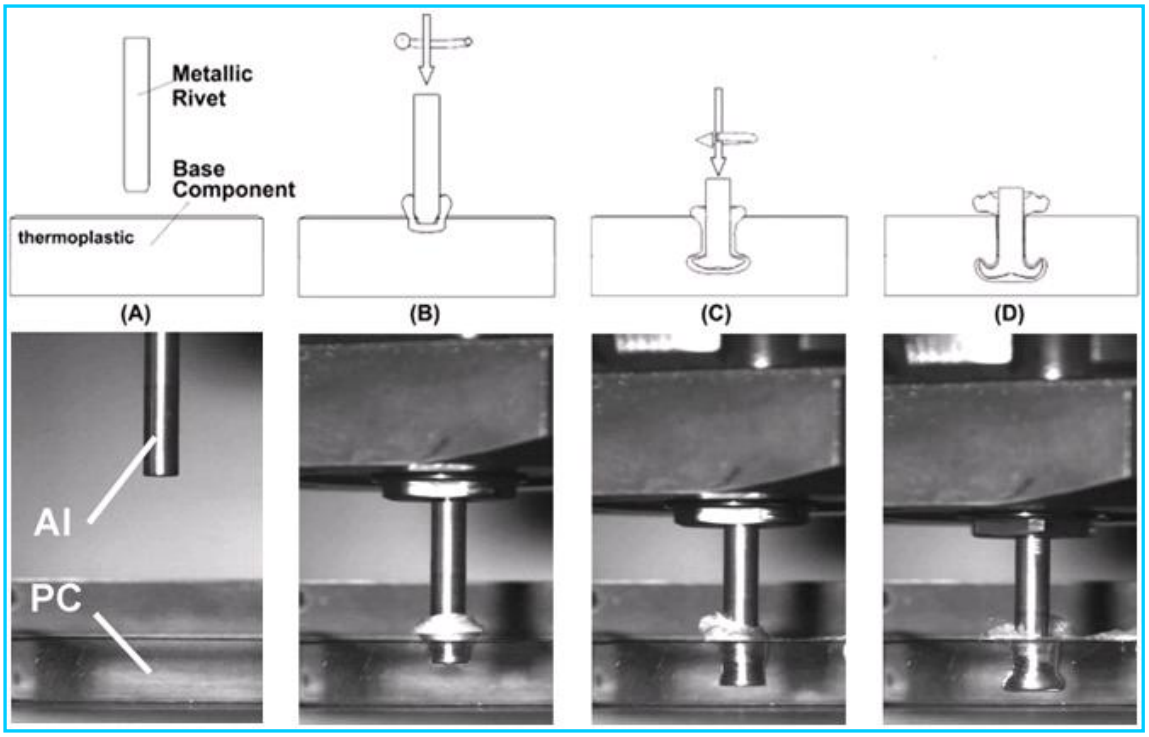

Figure 3 – Schematic view of the FricRiveting process. (A) Positioning of the joining partners, (B) Feeding of the rivet into the polymer (Friction), (C) Rivet forging, (D) Joint consolidation [18]. The main steps can be better visualized on a polycarbonate / aluminum riveted joint with the process filmed with a high-speed camera (courtesy of C. F. Rodrigues, HZG, Germany).

FricRiveting, winner of different innovation prizes worldwide, including IIW's Granjon Prize Category A in 2009 [19], was originally developed to join unreinforced thermoplastic by metallic rivets, but has the potential to fulfill the needs of the market of the composite/composite and polymer-metal multi-material structures by offering strong joints obtained in a simple, fast and more environmentally friendly way [17].

The equipment used for FricRiveting consists of a commercially available friction welding system. The use of adapted milling machines and robotic applications is also envisaged. Different joint geometries and material combinations are possible, including hermetic lap configurations on aluminum, titanium, polyetherimide, polyetherketone, polycarbonate and different polyolefines, among others. FricRiveting can be used in the production of metallic inserts in plastic products [12] and is being considered by the European aircraft industry to join of carbon fiber reinforced plastics parts [20]

2.2. Process parameters

The controllable input data of the joining equipment represents the process parameters. The main process parameters of FricRiveting are the Rotational Speed (RS), Joining Time (JT) and Joining Pressure (JP). The Rotational Speed represents the angular velocity of the rotating cylindrical rivet and is the main parameter affecting the temperature development, controlling also the viscosity of the molten polymer and thermo-mechanically induced physical-chemical changes in the polymer (e.g. thermal defects and degradation). The Joining Time has two components: Friction Time (FT) and Forging Time (FOT). The joining time influences the level of volumetric defect formation related to the thermo-mechanical processing; it controls the amount of heat energy supplied to the molten polymeric film. The Joining Pressure has also two components, related to the ones of the joining time: Friction Pressure (FP) and Forging Pressure (FOP). The main role of the Joining Pressure is to control the rivet forging and consolidation phases and is related to the normal pressure distribution on the rubbing surfaces of the joining partners [18].

2.3.Advantages and limitations of FricRiveting

Friction Riveting combines the advantages of mechanical fastening and welding and with an adequate design of the joint the benefits of this innovating process are [21]:

- Little or no surface preparation needed
- No obligatory pre-through holes in the polymeric plates, leading to less stress concentrations
- Hermetic sealed joints can be created
- Joining is independent of position (horizontal / vertical)
- Reduced number of process steps and short joining cycles, providing the potential of cost savings
- A wide range of materials can be joined
- Simple and low cost commercial available machinery
- Robotic applications are possible
- Good joint tensile and shear mechanical performance

The process is directly applicable to thermoplastic polymers only; a minimum working thickness of the joining partners is needed; friction-riveted connections cannot be disassembled and only spot-like joints can be achieved.

3. Materials and Methods

3.1. Materials

Different materials combinations were evaluated in course of this project including commercially available aluminum and titanium alloys and GFRP laminates. This paper reports only a selected combination thermoplastic glass fiber reinforced laminates/titanium/aluminum shoe joint that could be also used in other structural engineering applications, such as in aeronautics and automotive. For the complete study, please refer to [2].

3.1.1. Glass fiber reinforced polyetherimide (PEI-GF)

Glass-fiber-reinforced polyetherimide laminated sheets (PEI-GF, Figure 4) with a thickness of 6,2 mm were selected as structural-element composite material. The PEI-GF composites (TenCate Advanced Composites) were manufactured by plying up 28 plies (ply stacking sequence [0º, 90 º]), at a ply thickness of 0,24 mm per ply. PEI-GF is a high strength, chemical and heat resistant composite, used mostly in the aerospace industry, for structural and interior applications, paneling and other industrial or recreational applications [22]. The mechanical properties of PEI-GF are presented in Table 1:

Table 1 - Mechanical properties of PEI-GF [23]

Property	Charactertistic value		units
	Warp	Weft	
Density	1.91		g/cm³
Tensile strength	484	445	MPa
Tensile modulus	26	24	GPa
Compression strength	727	676	MPa
Compression modulus	29	27	GPa
In-plane shear strength	129		MPa

The polyetherimide resin content of the composite is situated at 50% in terms of volume and 33% by weight. PEI-GF has a glass transition temperature (Tg) of 210ºC and a thermal conductivity of 0.22 W/m-K. PEI is an amorphous polymer.

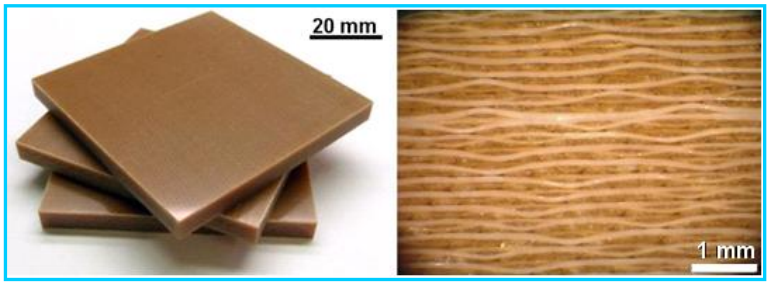

Figure 4 - PEI-GF specimens (left) and
cross - sectional microscopic view (right)

3.1.2. Titanium rivets

M5-thread rivets (pitch of diameter 4,6 mm) with the length of 60 mm were fabricated with extruded titanium grade 2 rods. The nominal chemical composition of this alloy is presented in Table 2:

Table 2 – Nominal chemical composition of Titanium grade 2 [24]

Wt%	C	H	Fe	N	O	Ti
	≤ 0.10	≤ 0.015	≤ 0.30	≤ 0.030	≤ 0.25	bal.

Titanium grade 2 is a commercially pure titanium alloy with high strength, high specific strength and good corrosion resistance. Table 3 summarizes the main properties of the rivets used in this work. It is usually applied in the automotive, aerospace or chemical plant industries. It has a density of 4,51 g/cm³ and a thermal conductivity of 16,4 W/mK. Its melting point is at 1665 ºC [20].

Table 3 – Main properties of Titanium grade 2 [24]

ASTM grade	Mechanical properties			Thermal properties
	Tensile strength, ultimate (MPa)	Tensile strength, yield (MPa)	Thermal conductivity (W/m-K)	Melting point (ºC)
Titanium grade 2	344	275	16.4	1665

3.1.3. Aluminum AA 2198 plates

AA 2198-T851 sheets of 3 mm thickness were used for the lap shear specimens in order to simulate the role of the gusset in the future bridge truss girder connections. The AA 2198 alloy has Al, Mg, Cu and Li as main alloy components. The lithium content offers the advantage of lower density compared to common Al alloys and an increase in elasticity modulus. The rolled sheets used in this work were previously characterized by Pieta and dos Santos [25], with the resulting chemical composition displayed in Table 4.

Table 4 - Chemical composition of Aluminum AA 2198-T851 [25]

Wt%	Fe	Cu	Li	Mg	Mn	Ag	Si	Ti	Zr	Al
nominal	0.04	3.40	0.80	0.27	0.04	0.18	0.03	0.03	0.10	bal.

3.2. Methods

3.2.1. Joining equipment and procedure

The friction riveting equipment used at the Helmholtz Zentrum Geesthacht (HZG) consists of a high speed friction welding system RSM 400 (Harms & Wende GmbH & Co. KG, Hamburg, Germany). The modular friction welding system is able to operate with rotation speeds of 6000 – 24600 rpm, axial pressures of up to 1.0 MPa with rivets up to ø 14 mm. Figure 5 shows the whole ensemble of the welding system together with the experimental frame. Prior to riveting, joining partners were cleansed with acetone to remove machining fluids.

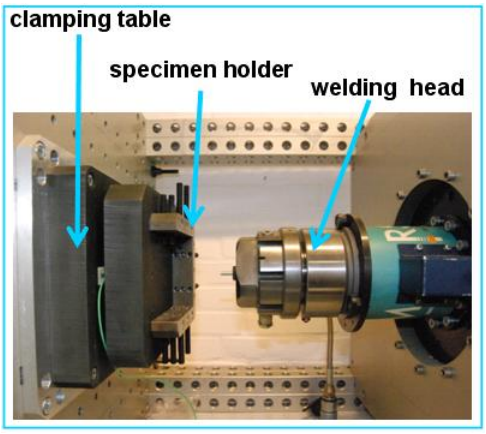

Figure 5 – RSM 400 welding system used for FricRiveting

3.2.2. Microstructural Properties

In order to analyze the microstructure of the joints, stereo microscopy and light optical microscopy (LOM) were chosen. Standard metallographic preparation was applied to specimens' cross sections extracted from the centre of the rivet across the whole joint thicknesses, with a diamond low speed saw and embedded in low cure temperature epoxy to avoid thermal changes in the polymer matrix.

3.2.3. Joint mechanical performance

Lap shear tests were carried at a strain rate of 2 mm/min at room temperature (21°C) in a 100 kN Zwick/Roell universal testing machine. Lap shear specimens were cut following the dimensions prescribed by ASTM D 5961 M – 08 [26]: 135 x 36 x 6.2 mm, overlap of 36 mm, a free rivet length 12 mm (spindle clamping length of 50 mm) and Φ 5 mm rivet nominal diameter (M5-threaded rivets). Lap shear specimens were constituted of PEI-GF base plates with friction riveted threaded Ti gr.2 rivets (M5) (Figure 6A) and an aluminum plate (AA 2198 alloy), perforated with a through-hole diameter of 5 mm. Hole edges were chamfered at a 90° angle for reducing stress concentrations. The friction riveted PEI-GF plates and the AA2198 plates assembled together using stainless steel M5 nuts and washers with a clamping force of 5 Nm, as shown in Figures 6A to 6C.

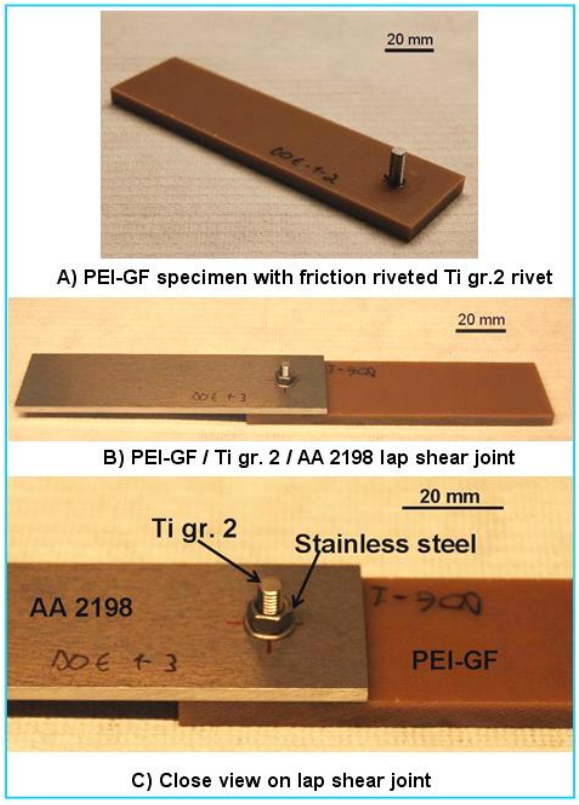

Figure 6 – Assembly procedure of the lap shear specimens: A) titanium rivets are inserted in the PEI-GF composite plate; B) the perforated Al-plate is overlapped onto the riveted composite element and finally the washer and nut are added with a torque tool.

3.2.4. Process optimization and statistical analysis

Design of experiments (DOE) and analysis of variance (ANOVA) were used to evaluate process mechanical performance. Ultimate lap shear force (ULSF) was selected as the response to process optimization via the Taguchi method. In the Taguchi method, pairs of parameters combinations were tested using the orthogonal array experimental design proposed by Taguchi [27].

Friction pressure was set constant to 0.6 MPa, because it has been demonstrated to have a very weak influence on heat generation [18]; The levels of the other joining parameters were varied. Thus, only the influence of the four remaining parameters was studied in the Taguchi-L9 (34) DOE, each at three different levels:

- RS: 8000, 10000, 12000 rpm
- FT: 700, 1200, 1500 ms
- FOT:1200, 1850, 2500 ms
- FOP: 0.6, 0.7, 0.8 MPa

This powerful statistical tool allows the reduction of material consumption and experimental time [28] by decreasing the number of experiments. In the current work, with four parameters (RS, FT, FOT and FOP) and three levels (minimum, medium, and maximum), the proper array is L9, with a number of nine parameter combinations, corresponding to nine experimental joining conditions, as shown in Table 5.

Table 5 - Taguchi-L9 orthogonal array - lap shear tests of PEI-GF/Ti gr.2/Al 2198 FricRiveting overlap joints

Joining Condition	Rotational Speed [rpm]	Friction Time [ms]	Forging Time [ms]	Forging Pressure [MPa]
1	8000	700	1200	0.6
2	8000	1200	1850	0.7
3	8000	1700	2500	0.8
4	10000	700	1850	0.8
5	10000	1200	2500	0.6
6	10000	1700	1200	0.7
7	12000	700	2500	0.7
8	12000	1200	1200	0.8
9	12000	1700	1850	0.6

Each experiment had a number of four replicates. For determination of the effect of each variable (parameter) on the output, the signal-to-noise ratio (S/N ratio) a statistical parameter expressing the quality of the measurement [29] was calculated for each experiment.

3.2.5. Temperature measurement

The temperature measurement system (Figure 7) consisted of an infrared thermo camera (High-end Camera Series ImageIR, Infratech GmbH, Germany), connected to a computer with data collection and processing software (IRBIS 3 Professional). Specimens were painted with black ink in order to increase emissivity and reduce measurement noises. The temperature was recorded during joining, from the expelled polymeric matrix material, on the contact area between rivet and polymer; because of the low thermal conductivity of the

polymer, one can assume that the measured average temperature in the softened flash material is nearly the same as in the molten layer of polymer around the plasticized rivet tip [18].

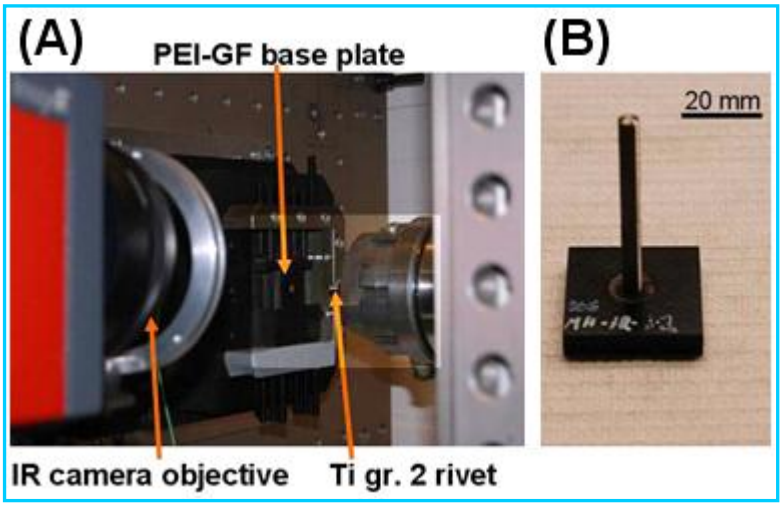

Figure 7– A) Experimental setup for infrared temperature measurement. B) friction-riveted specimen after joining.

4. Results and discussions

4.1. Feasibility study: FricRiveting of PEI-GF / Titanium grade 2

4.1.1 Temperature history

Figure 8 shows the average peak temperatures monitored during this study. Process temperature varied between 450 ºC and 560 ºC. The recorded temperatures for all tested specimens were situated at 30-40% of the titanium grade 2 melting point (1665 ºC). In the case of titanium, increased temperatures lead to a higher ductility, therefore a higher formability. The temperatures for hot forming of commercially pure titanium range from 480 ºC - 705 ºC [30]. The measured temperatures of the DOE-specimens were in this range, explaining thereby the achieved formation of the rivet anchoring zone. With joining times in FricRiveting of less than 5 seconds, there is no risk of scaling and embrittlement of the titanium due to long-time exposure to extreme temperatures, as recommended in literature. The recommendation to avoid temperatures over 815 ºC in order to limit the risk of deterioration of the mechanical properties is also fulfilled [30].

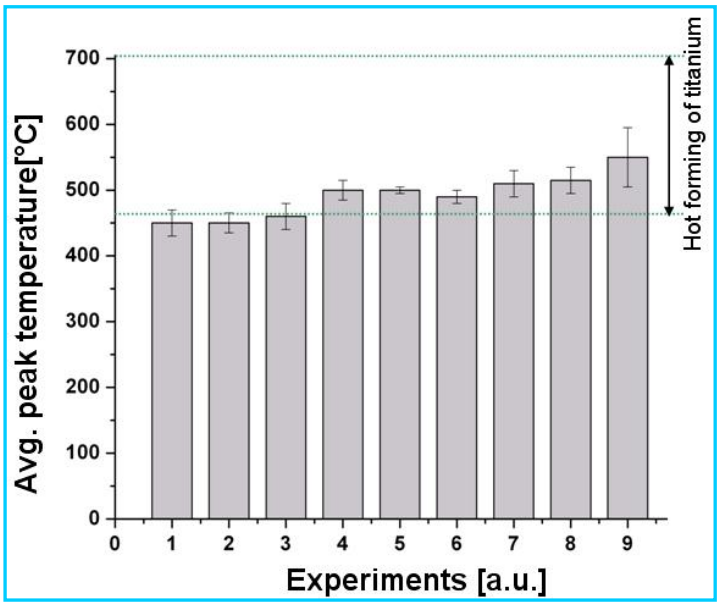

Figure 8 – Monitored average peak temperatures

Furthermore extensive thermal degradation of the PEI matrix is not expected. Friction riveted joints on unreinforced PEI produced with similar joining parameters, leading to similar peak temperatures and exposures times, were reported to suffer less thermo-mechanically induced degradation [18, 31]. This can be attributed to PEI's high thermal-resistance; this thermoplastic displays accelerated susceptibility to thermal degradation only at temperatures above 600 ^{o}C and long exposure times [31], which were not measured in this work.

Recently published work [18, 19] on unreinforced PEI aluminium rivets joined by FricRiveting addressed the importance of the rotational speed and joining time on heat generation. Selected results on the influence of the rotational speed on heat generation will be used to illustrate the temperature development during friction riveting of PEI / Ti gr.2 specimens.. Three conditions with 8000 rpm, 10000 rpm and 12000 rpm were compared (FT = 700 ms, FOT = 18500 ms, FP = 0.6 MPa, FOP = 0.8 MPa). Table 6 summarizes the results of the peak temperatures for the specimens under investigation. Figure 9 shows an example of an infrared thermogram and the average curve for the temperature measured; average peak temperature results were obtained within the marked area containing the expelled flash material.

Table 6 - Influence of the rotational speed on the peak temperatures (average of two measurements) in PEI-GF/Ti Gr.2 FricRiveting joints

Experiment	Rotational Speed [rpm]	Avg. Peak Temp. [^{o}C]
T1	8000	450 ± 25
T2	10000	550 ± 30
T3	12000	600 ± 35

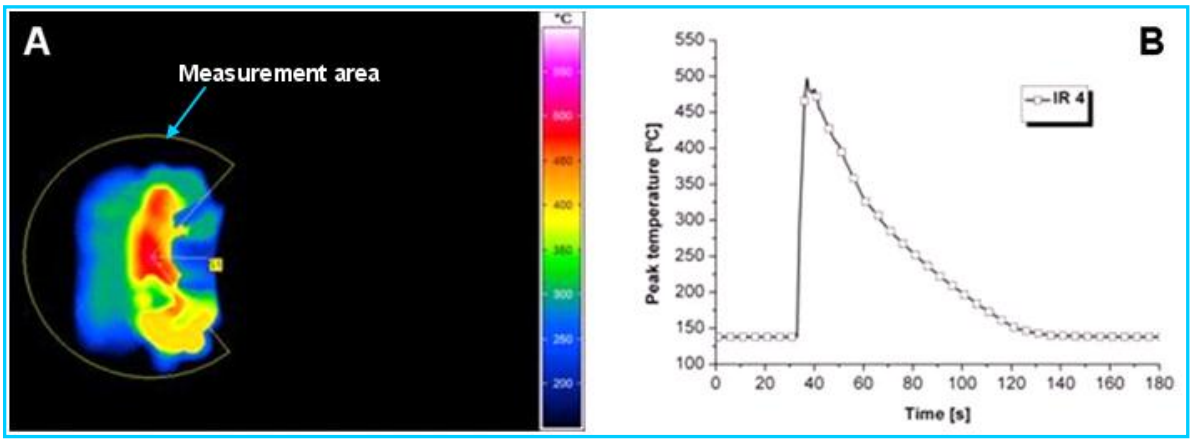

Figure 9 - (A) Infrared thermogram showing the temperature of the softened composite flash material being pushed off to the surface. (B) The average peak temperatures measured from the semi-circle area in (A). (a replicate specimen for condition T2).

4.1.2. Microstructural evolution

Joints were successfully produced within the following parameter ranges: rotational speed of 6000 - 20000 rpm, joining times of 1.9 – 4.2 s and joining pressures of 0.6 – 1.0 MPa. Typical cross-sectional views through the centre of PEI-GF / Ti gr.2 rivet-insert type joints are shown in Figure 10. The formation of the anchoring zone (the deformed tip of the rivet) can be observed; only few volumetric thermal flaws could be identified using light optical microscopy.

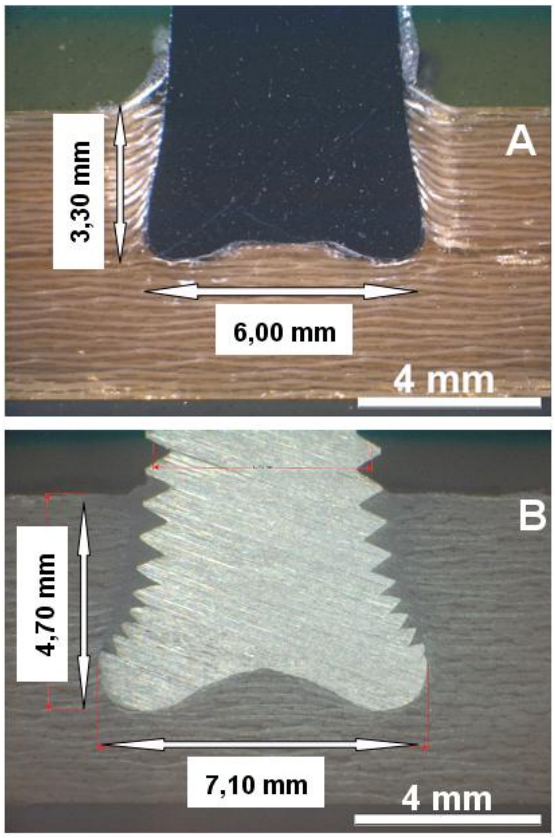

Figure 10 – Examples of cross-sectional views for (A) a friction-riveted PEI-GF/Ti gr.2 plain rivet joint (RS = 10000 rpm, FT = 700 ms, FOT = 2500 ms, FP = 0.6 MPa, FOP = 1.0 MPa) and (B) a friction-riveted PEI-GF/Ti gr.2 M5-threaded rivet joint (RS = 10000 rpm, FT = 700 ms, FOT = 1200 ms, FP = 0.6 MPa, FOP = 0.7 MPa)

During insertion, rivet perforates the glass fiber woven, while pieces of broken fibers and molten PEI matrix are expelled as flash material. The glass fiber woven around the rivet is not burned, but shifted in the direction of the polymeric material flow to about 45 degrees, while it largely remains in contact with the rivet shaft after the consolidation of the molten polymeric layer [2]. Figure 11 presents the overview of the metallographic cross-sections of the studied specimens. The detailed analysis of the joint microstructure was out of the scope of this work. Further information on the microstructural zones and thermo-mechanically induced transformations in friction riveted joints can be found elsewhere [19].

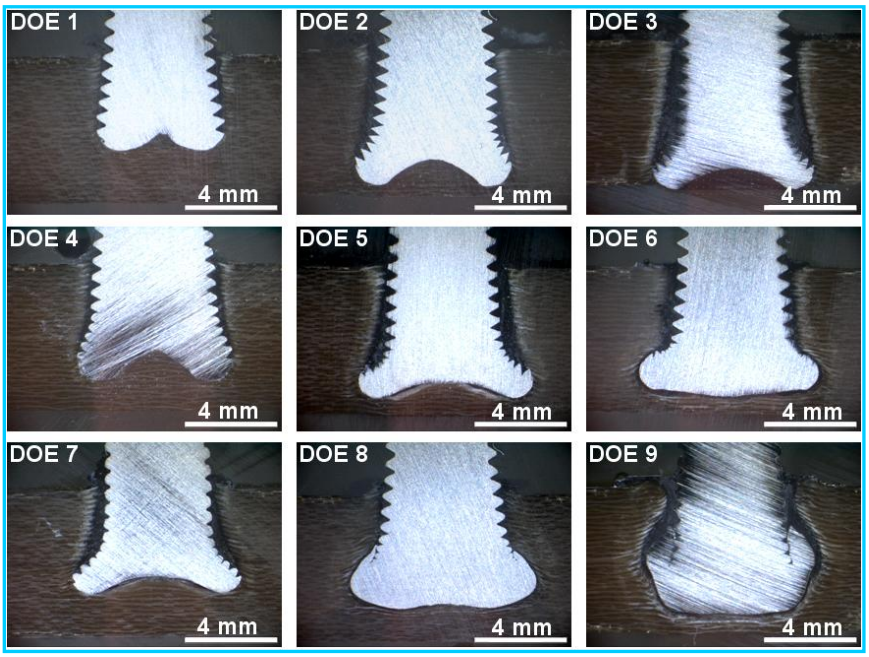

Figure 11 – Overview of metallographic cross sections for Taguchi L9 joint conditions.

4.2. Lap shear testing of PEI-GF/AA 2198/Ti Gr.2 hybrid joints

Table 7 presents the results of the Taguchi-L9 experiments with the response ultimate lap shear force (ULSF) chosen for the statistical evaluation.

Table 7 - Experimental results for Taguchi-L9 – Ultimate lap shear forces of PEI-GF/AA 2198/Ti gr.2 joints for four replicates per experimental condition

Experiment	ULSF 1 [N]	ULSF 2 [N]	ULSF 3 [N]	ULSF 4 [N]	Average ULSF [N]	ULSF Standard Deviation [N]
1	4000	3930	2300 *	4980	3800	1110
2	5050	3800	5500	3700	4500	900
3	4250	3140	2910	3850	3500	621
4	4990	4915	4600	5800	5000	511
5	5370	5070	3700	3500	4400	947
6	3320	3850	3100	3830	3500	375
7	4800	4050	5430	5900	5000	802
8	3950	4090	4680	4060	4200	329
9	3810 *	4870	4400	4400	4400	434
* Specimens failing in the metallic rivet by bearing						

Amancio-Filho [19] reported the occurrence of two the different failure mechanisms under static shear loading for friction riveted lap joints on unreinforced PEI. Amancio-Filho study, lap joints were tested without the application of nuts and washes; due to the reduced rivet clamping force, bearing failure took place on the upper plate, while secondary bending increased stress concentration around the anchoring zone. Final joint failure took place by net-tension, with cracking propagating through the thickness of the lower plate.

Two final failure modes were observed in this study. From the 36 tested specimens, only two (marked in the Table 7) failed through bearing failure type in the polymeric plate, where rivet was pulled out from the lower plate. The remaining specimens failed by shearing of the shaft of the metallic rivet. An example of the two different final failure modes can be observed in Figure 12. Although bolt torque was carefully applied during the assembly of the connections, the probable explanation for the different behaviour of the two mentioned specimens was associated to insufficient clamping force leading to changes in loading distribution resulting in premature joint failure. Further analysis of the micromechanical failure mechanisms is needed in order to better understand these results

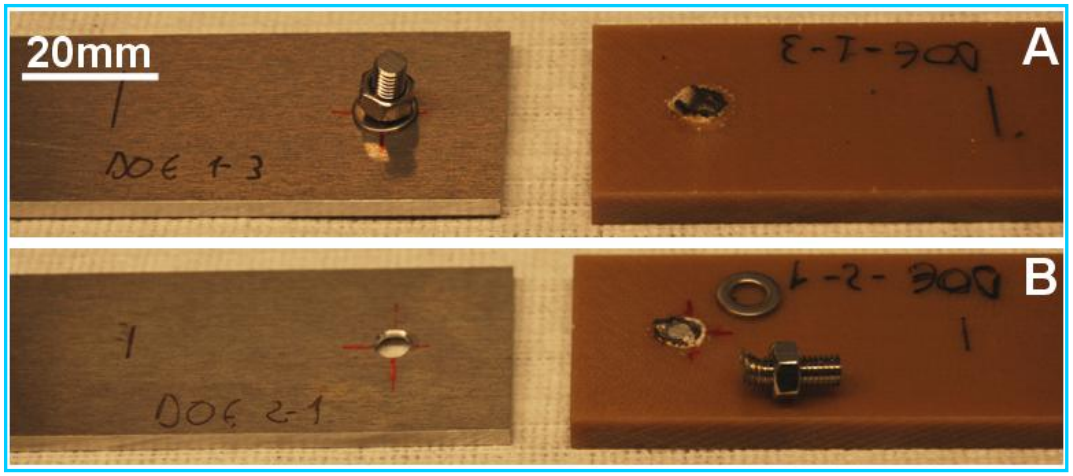

Figure 12–Final failure modes. A) Bearing failure in lap-shear specimen - Condition 1, replicate 3 (RS= 8000 rpm, FT= 700 ms, FOT= 1200 ms, FP=0.6 MPa, FOP 0.6 MPa)
B) Rivet shear failure in lap-shear specimen - Condition 2, replicate 1 (RS= 8000, FT= 1200 ms, FOT= 1850 ms, FP= 0.6 MPa, FOP= 0.7 MPa)

The ultimate lap shear strength (ULSS) of the joints can be addressed as the nominal and actual strength. The nominal ULSS can be expressed as the ratio between the ultimate lap shear force and the nominal area of the hole for each friction riveted joint. The nominal area

of the hole can be simplified calculated as the coupon's thickness times the nominal diameter of the hole, as addressed by ASTM D 5961 M-08 [26] and indicated in Equation 1.

$$R = \frac{F}{t \cdot d} \tag{1}$$

, where R – simplified lap-shear strength

F – the ultimate lap shear force

t – coupon thickness

d- nominal diameter of the hole

By following the same assumptions, the actual ULSS can be calculated with the real cross-sectional area of the hole created by the deformed rivet inserted into the coupons (see schematic representation in Figure 13), by the following equation:

$$R_{real} = \frac{F}{A_d} \tag{2}$$

, with A_d - the real measured area of the hole created by the deformed rivet

The calculated values of the nominal and actual ultimate lap-shear strengths (ULSS) achieved in the experiments are listed in Table 8. In the calculation of the nominal ULSS, the pitch diameter of the M5-threaded rivet (4.6 mm [32]) and the thickness of PEI-GF (6.2 mm), the thickest coupon in the assemble joint, were used for simplification purposes. The real areas for the calculation of the actual ULSS were obtained from graphical measurements on metallographic cross-sections, as schematically shown in Figure 13.

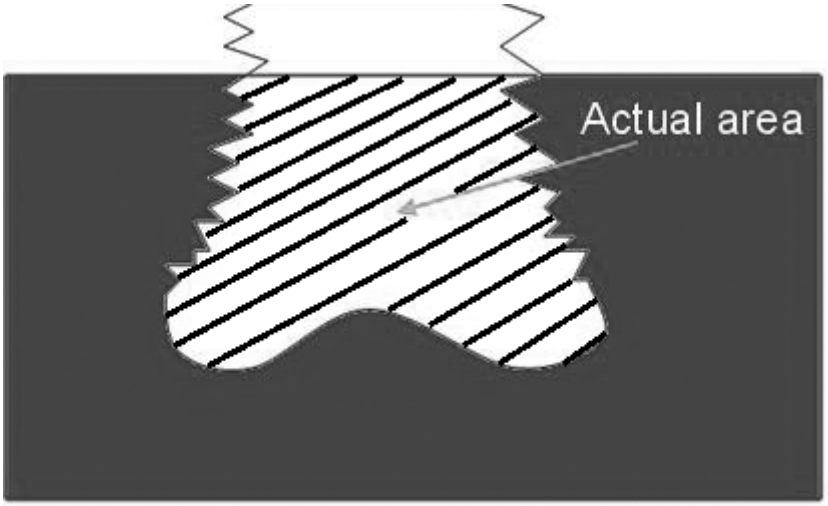

Figure 13 - Scheme of actual area used for the determination of the actual ULSS

Table 8 - Nominal and actual ultimate lap shear strengths of PEI-GF/AA2198/Ti gr.2 joints

Experiment	Average ULSF [N]	Nominal ULSS [MPa]	Real ULSS [MPa]
1	3800	132.00	178.40
2	4500	156.25	168.00
3	3500	121.50	100.00
4	5000	173.60	178.60
5	4400	152.80	145.00
6	3500	121.50	100.00
7	5000	173.60	199.20
8	4200	145.80	126.50
9	4400	152.80	122.20
Avg.	**4275**	**147.80**	**146.40**
StD.	**576**	**19.7**	**38.95**

From the table it is possible to see that both nominal and real ULSS specimens have comparable average ULSS values (an average difference of 21.0 MPa).

The PEI-GF/AA 2198/Ti gr.2 hybrid joints could achieve shear strengths up to 70% of the tensile resistance of the M5-metallic rivet (see Table 3) and about the same level as in-plane shear strength of the composite PEI-GF base plate (see Table 1).

4.3. Statistical evaluation of the results

The main effects plots for the means and signal-to-noise ratios (S/N) for ultimate shear force can be seen in Figure 14 and Figure 15, where the forging time (FOT) resulted as the main parameter influencing the results, followed by the friction time (FT) and Rotational Speed (RS).

This can be concluded from the slopes of the curves for the main effect and S/N ratio curves. The steeper the slope the higher will be the influence of one parameter in the respective response. One can affirm thereby that the joining time (JT) represented by the components FT and FOT and the Rotational Speed (RS) are the parameters with the largest influence on the lap-shear strength in the studied materials combination.

This behaviour was reported to be associated with changes in heat input, whereby larger RS and JT resulted in larger heat generation [18]. This was also observed in this work

for the evaluation of the process temperature (see Table 6). Increased temperatures improve rivet plasticizing and consequently the deformation and insertion depth of the anchoring zone. This phenomenon was also observed for the current joints but published in a separate document [2]. This investigation indicated that, the higher the deformation and insertion depth of the rivet the larger the rivet anchoring performance is, leading to stronger joints.

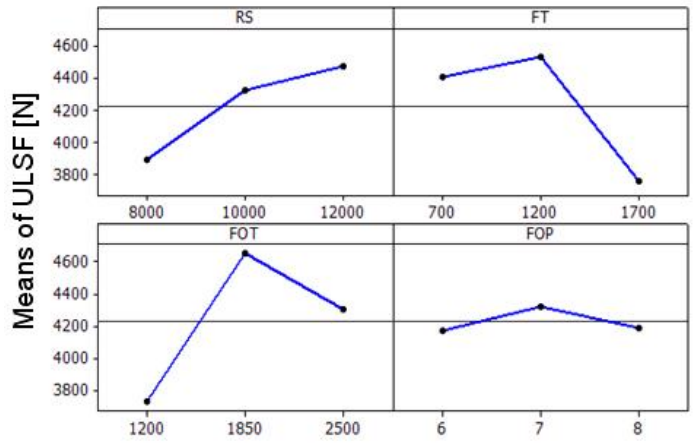

Figure 14 – Main effect plots for the means of ultimate lap shear forces (ULSF) of the friction rivet joints in the Taguchi-L9 design of experiments.

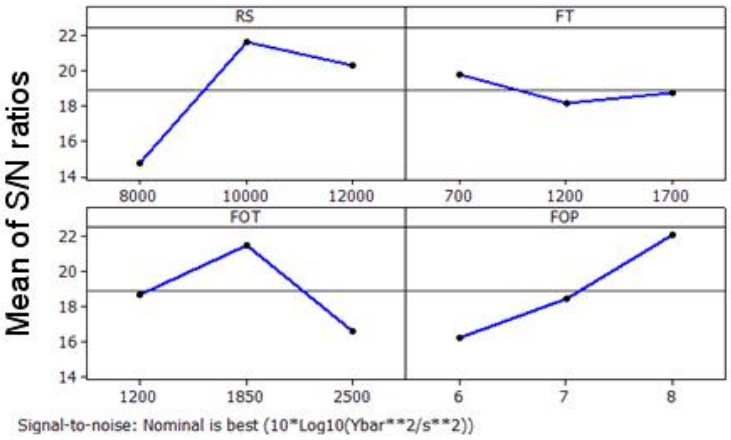

Figure 15 – Main effects plot for S/N ratios for the ultimate lap shear forces (ULSF) of the friction rivet joints in the Taguchi-L9 design of experiments.

The model was validated by predicting the ULSF for four complementary conditions, selected within the parameters range of the Taguchi-L9 array as recommended in the literature [29]. The validation conditions with their predicted and experimental average ULSF are presented in the graph in Figure 16.

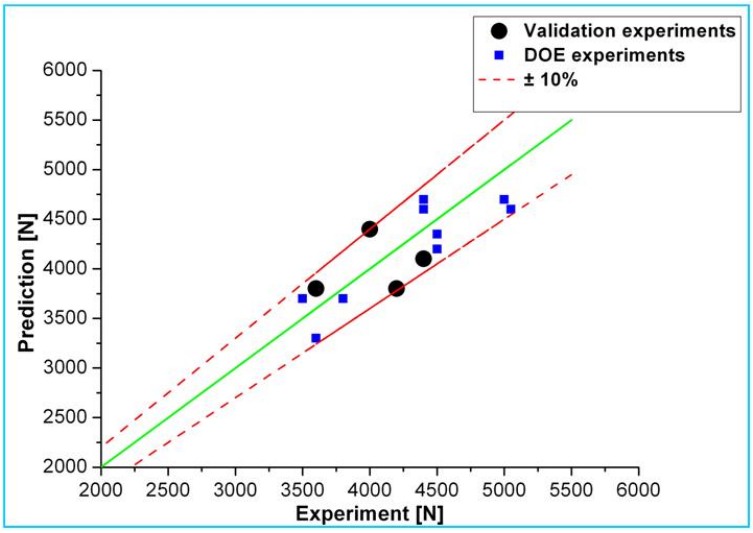

Figure 16 – Validations for the design of experiments

As generally accepted by the polymer and composite welding community, a deviation of 10% is considered normal, usually due to the variations in the base material properties. Considering that the model error varied from 6.0% to 9.1 % the model can be considered statistically valid.

4.4. Comparison with bolted joints

In order to compare the mechanical performance of friction-riveted joints with state-of-the-art fastened joints, bolted lap-shear specimens (Figure 17) were produced analogically to the friction riveted lap-shear specimens, with identical materials and specimen geometries, and tested according to the same standards.

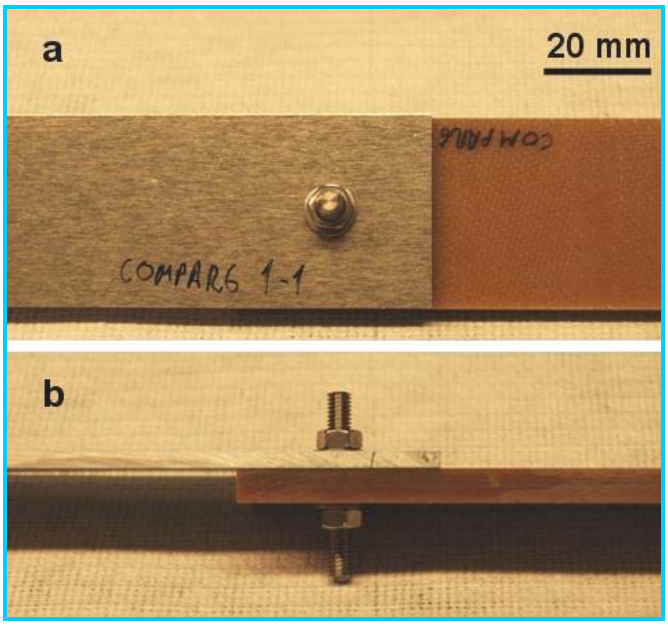

Figure 17 – Bolted lap-shear configuration on PEI-GF/Ti gr.2/ AA 2198 for comparison analysis. a – plane view, b – side view

Average ULSF of 4360 ± 600 N was achieved for the bolted connections, corresponding to an average nominal ULSS of 141.0 ± 20MPa, nearly similar to the ones of the friction riveted specimens (147.8 ± 19.7 MPa). All bolted specimens failed by the shear of the metallic rivet shaft as shown in Figure 18.

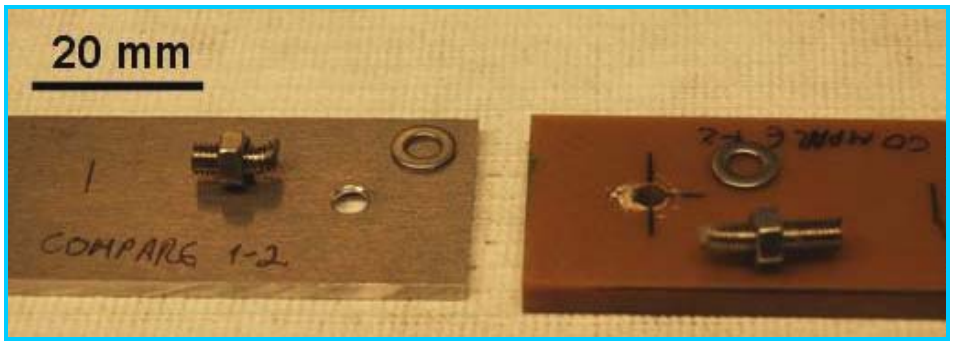

Figure 18– Aspects of the fractured bolted comparison specimen showing rivet shear failure mode.

Figure 19 compares the average mechanical strength of all the friction-riveted specimens together with the bolted joints. From the graph, one can observe that the friction riveted lap joints investigated in this work have comparable or better strength and as bolted lap; under optimized conditions (Experiment 7) friction-riveted overlap joints could achieve lap shear strengths of up to 20% higher than bolted connections (Experiment 7, see Table 5).

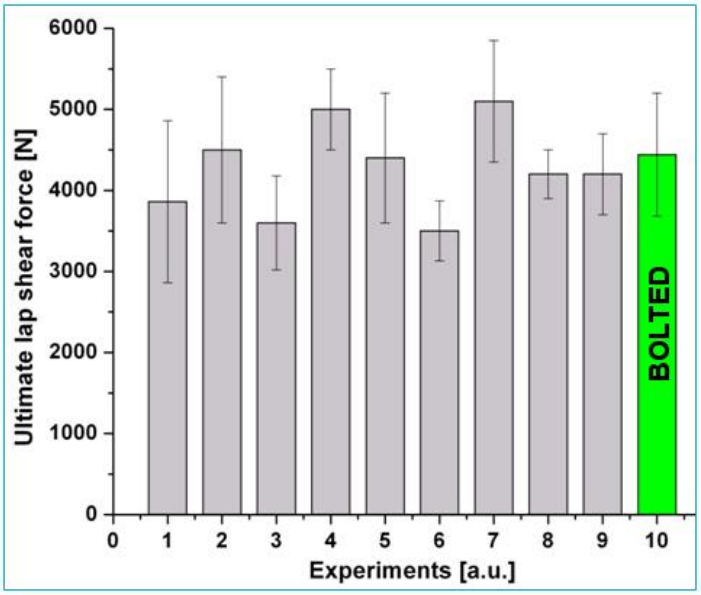

Figure 19 – Average ultimate lap-shear force results for DOE experiments and bolted joints

5. Case study: GFRP lightweight emergency bridge

5.1. GFRP lightweight emergency bridge

A 25m-span Warren truss bridge (Figure 20) was calculated using the SAP2000 v14 Computers and Structures finite element software in order to obtain the values of the axial forces in a presumptive real truss GFRP emergency bridge made of PEI-GF profiles. The maximum axial forces were assumed to be transmittable through the joints in the finite element bridge model. The calculus of the bridge was not intended for stability verification, as it is not the scope of this work [2].

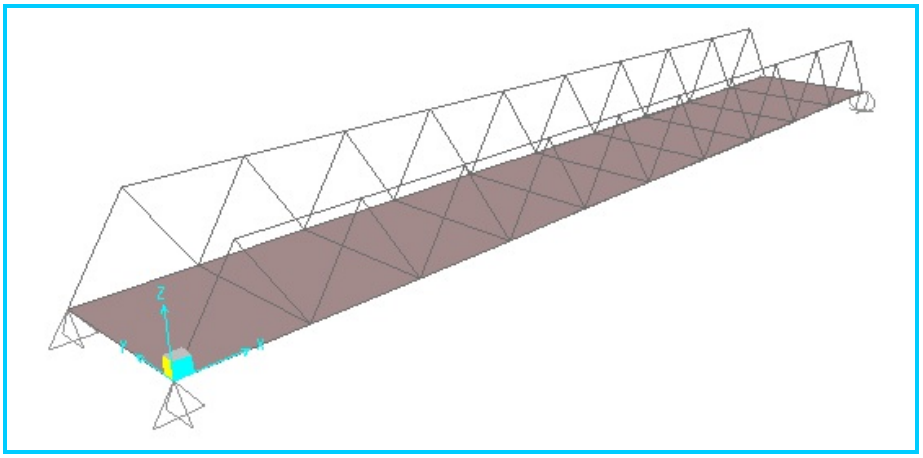

Figure 20 – Isometric view of the PEI-GF truss bridge with friction-riveted profiles modelled in this study

The cross section shapes of the truss elements were chosen similar to commercially available shapes of structural profiles (Fiberline Composites A/S, Denmark [33]). For practical reasons in order to ensure an easy exchange of truss members only three different types of profiles have been proposed to be used in the bridge model (Figure 21):

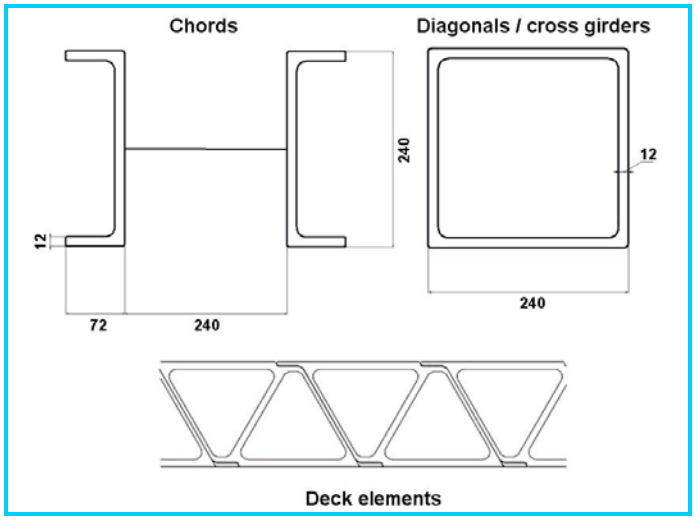

Figure 21 – Structural profiles proposed for GFRP lightweight bridge model

With the proposed profiles the whole structure would weight approximately 15 tonnes, from which around 10 tones is the dead load of the bridge deck. The live load of the bridge consists of a single 30 tonne truck from the standard A30 convoy [34]. The crossing speed of the truck is set to 40 km/h, with a dynamic impact factor of 1.2. The width of the bridge carriageway is 3900 mm, assuring a single lane for the vehicle crossing (width of the A30 convoy is 2700 mm). For the main load combination (dead load + live load from A30 truck) the maximum axial force was determined in the central members of the lower chords, to be around 760 kN, as presented in Figure 22.

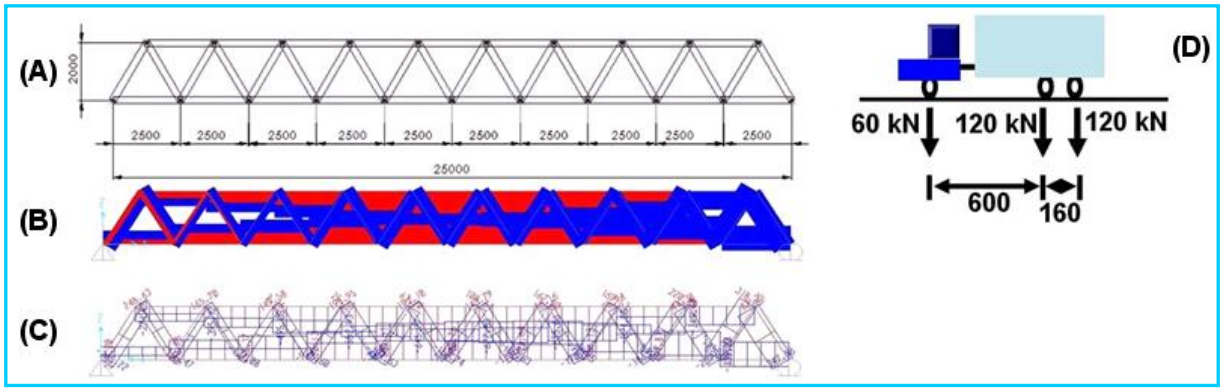

Figure 22 – (A) Static model of the bridge. (B) Evolution of axial forces under mobile loads. (C) Maximum axial forces. (D) A 30 standard truck with loads

5.2. Friction-riveted connections for GFRP truss elements

A knowledge-based friction-riveted joint geometry was proposed for the connections of the truss elements in the bridge model. In a first step, threaded titanium grade 2 rivets are inserted by FricRiveting in the adjacent GFRP bar, as shown in Figure 23.

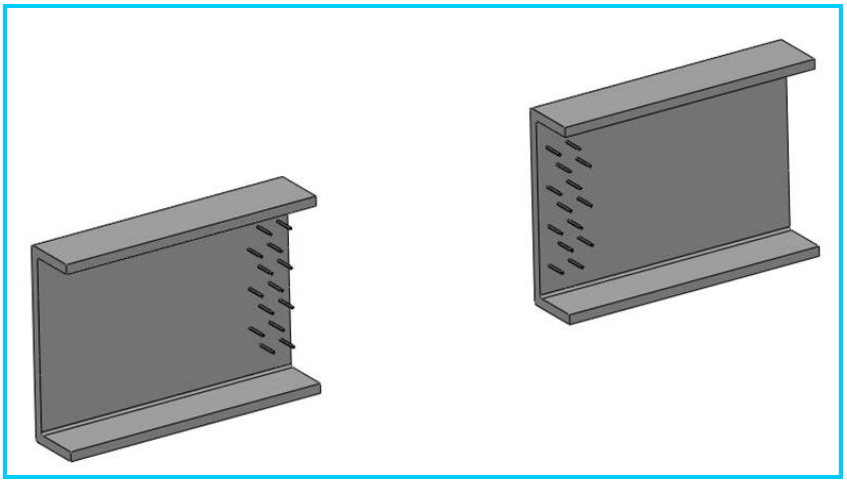

Figure 23 – Scheme of the insertion of friction-riveted GFRP elements.

The load transfer was calculated by using 3 mm thick pre-drilled aluminium gussets; subsequently, the gussets a connected the friction-rived GFRP bars, fixed by nuts and washers (Figure 24). Figure 25 shows the scheme of an assembled GFRP profile connection by the screwed aluminium gusset.

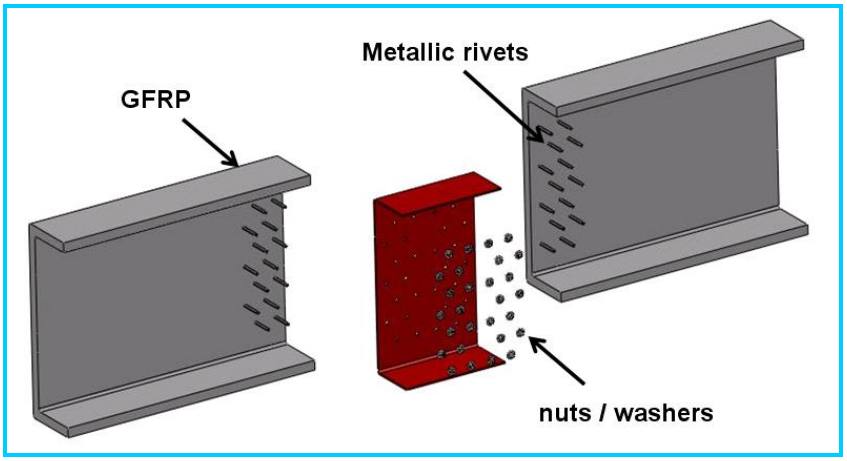

Figure 24 – Joining partners used for the structural analysis.
(GFRP structural profiles, metallic rivets, aluminium gusset, metallic nuts and washers)

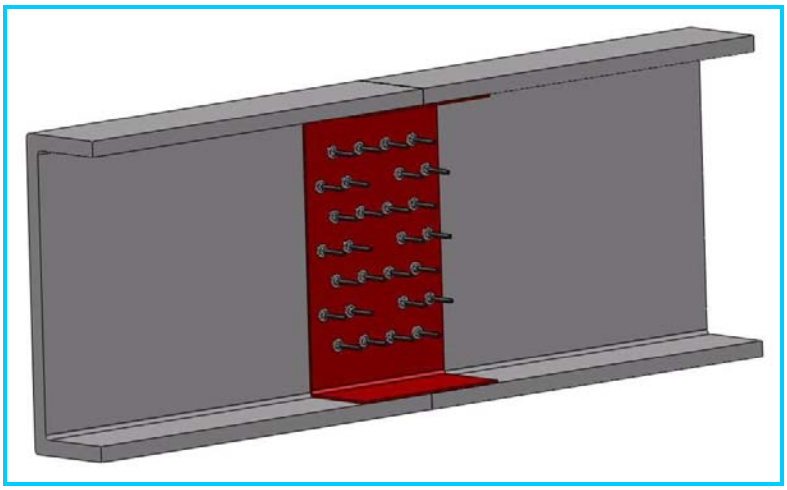

Figure 25 – Schematic view of the assembly on GFRP/Ti gr. 2 /AA 2198 friction riveted joints used in the structural bridge model.

The connections were calculated using the lap-shear strength from the DOE evaluation, with the highest value of 200 MPa from condition 7 joining conditions (Table 8). In the case of the highest joint force to be transmitted (760 kN), the number of rivets necessary was determined, using the following equation [35]:

$$n \geq \frac{F}{\frac{\pi \cdot d^2}{4} \cdot \tau_s} \qquad (2)$$

With: n – number of rivets

F – force to be transmitted

d – rivet diameter

τ_s - shear strength of the rivet (based on the optimized results of the DOE)

With the tested nominal rivet diameter of Ø 5 mm, Equation 2 specifies a number of 162 rivets necessary for the GFRP/Al/Ti rivet assembly. Although at a first glance the calculated number of rivets appears to be elevated, this is accordance to values observed in riveted steel bridge nodes. It is expected that increasing rivet diameter would potentially reduce the amount of necessary rivets. However further investigations have to be undertaken on FricRiveting of PEI-GF with larger diameter rivets in order to confirm this assumption, as FricRiveting process variables are not linearly dependent to the rivet diameter.

6. Conclusions

This work demonstrated for the first time that thermoplastic glass fiber reinforced composite laminates can be joined by FricRiveting. The feasibility of FricRiveting on PEI-GF / Titanium / Aluminum connections for structural engineering applications was proven and investigated. Infrared thermography revealed that generated temperatures ranged between 450 ºC - 600 ºC. The measured peak temperatures were within the range of hot forming of titanium grade 2 (480 ºC – 705 ºC) indicating the formation of the rivet anchoring zone, but are smaller to 815 ºC, above which the alloy experiences detriments in its mechanical performance. Furthermore temperature was below the degradation range of the polyetherimide matrix (600 ºC). Considering the short joining cycles extensive thermal degradation is probably absent.

Microstructural characterization confirmed the formation of the rivet anchoring zone inside the composite base plate, with reduced amount of volumetric flaws. Overlap joints have been tested in order to investigate the behavior and lap-shear strength of friction riveted PEI-GF/Ti gr.2 / Al 2198-T851 joints; lap shear strengths of up to 200 MPa were thereby achieved The conducted design of experiments determined the optimal joining parameters for lap-shear strengths at the level of the shear-strength of the titanium alloy, causing in most of the cases final failure by shear of the metallic rivet. Comparison tests led to the conclusion that friction riveted overlap joints have similar to better (20 %, in optimized joints) mechanical performance and behavior as bolted joints.

Numerical modeling of a presumptive lightweight PEI-GF truss bridge showed that, if joined by FricRiveting, connections of composite bars assembled with aluminum gussets would require an amount of 162 rivets in order to transfer truss axial forces in the truss girder bars with calculated maximum stresses of 760 kN. An optimized geometry for friction-riveted PEI-GF/AA 2198/Ti gr.2 connections was proposed based on the knowhow generated in this work. This preliminary study showed the potential of the FricRiveting technique as an alternative, fast and cost-effective joining technology for future GFRP emergency bridges

Acknowledgments

The authors would like to acknowledge the financial support provided by the Helmholtz Association Germany ("Young Investigator Groups" programme – Grant "Advanced Polymer-Metal Hybrid Structures") and the Romanian Ministry of Labor, Family and Social Protection (Strategic Grant POSDRU 6/1.5/S/13 (2008), co-financed by the European Social Fund – Investing in People). L. Blaga is thankful to his PhD advisors, Prof. S. Amancio (Helmholtz-Zentrum Geesthacht) and Prof. R. Băncilă (Technical University of Timişoara) for their guidance in this work.

References

[1] C. Smallbone, M. Kocak, White Paper, Improving global quality of life through optimum use and innovation of welding and joining technologies, Edition 2012, International Institute of Welding

[2] L. Blaga, Innovating materials in bridge construction. Contribution to construction with composite fiber-reinforced materials, PhD thesis at the Technical University of Timisoara, Romania, ISBN 978-606-554-459-8, Ed. Politehnica 2012

[3] C. Tuatka, Use of FRP in bridge structures, MSc. Thesis in civil and environmental engineering at the Massachusetts Institute of Technology, June 2005

[4] L. Blaga, GFRP emergency bridges. An ecological lightweight solution, Proceedings of the workshop Sustainability of Constructions. Integrated Approach to Life-time Structural Engineering, COST Action C25, Timisoara, Romania, ISBN 978-973-638-428-8, 23-24 October 2009

[5] K.F. Koch, Hilfsbrücken. Grundlagen, Planung, Konstruktion, Ausführung, Werner Verlag, 1998

[6] Field Manual No. 5-277, Bailey Bridge, Headquarters Dept. of the Army, Washington DC, 9 May 1986

[7] M. LaViolette, Bridge Construction Practices using Incremental Launching, report of the Bridge Engineer Center, Center for Transport Research and Education, Iowa State University, Ames, 2007

[8] G. Sedlacek, M. Oppe, H. Trumpf, Design and testing of an inventive GFRP-truss-bridge for 40 t trucks and 30 m span, Proceedings of the COBRAE Conference 2005 – Bridge Engineering with Polymer Composites, Leusden 2005

[9] G. Sedlacek, H. Trumpf, Mobile Leichtbau-Festbrücke aus pultrudierten faserverstärkten Polymerprofilen, Bauingenieur, Springer VDI Verlag, Düsseldorf, Germany, 2005

[10] AASHTO, Standard specifications for highway bridges, Washington DC 2002

[11] R. W. Messler Jr., Joining composite materials and structures: some thought-provoking possibilities, Journal of Thermoplastic Composite Materials, Vol. 17, January 2004, Sage Publications, ISSN 0892-7057/04/01 0051

[12] L. Blaga, S. T. Amancio-Filho, J. F. dos Santos, R. Bancila, Fricriveting of civil engineering composite laminates for bridge construction, ANTEC 2012, Annual Technical Conferecnce Proceedings, Society of Plastic Engineers, Orlando FL 2012

[13] D. Duthinh, Connections of fiber-reinforced polymer (FRP) structural members: a review of the state of the art, NISTIR 6532, National Institute of Standards and Technology, Gaithersburg MD, US 2000

[14] L. C. Banks, Composites for Construction. Structural Design with FRP Materials, John Wiley & Sons, NY 2006, ISBN 0-471-68126-1

[15] J. T. Mottram, Y. Zheng, Further tests on beam-to-column connections for pultruded frames, Journal of Composites for Construction, 1999, ISSN 1090-0268

[16] S. T. Amancio-Filho, M. Beyer, J. F. dos Santos, US 7.575.149 B2: Method for connecting a metallic bolt to a plastic piece, US patent, 2009

[17] S. T. Amancio-Filho, J. F. dos Santos, Fricriveting: a new technique for joining thermoplastics to lightweight alloys, ANTEC 2008, Plastics: Annual Technical Conference Proceedings, Society of Plastic Engineers, Milwaukee WI 2009, ISBN 978-1-6056032-0-9

[18] S. T. Amancio-Filho, Friction Riveting: development and analysis of a new joining technique for polymer-metal multi-materials structures, PhD thesis at the Hamburg-Harburg University of Technology, GKSS 2007, ISSN 0344-9629

[19] S. T. Amancio-Filho, Friction Riveting: development and analysis of a new joining technique for polymer-metal multi-materials structures, Henry Granjon Prize Competition 2009, Welding in the World, Vol. 55, 2011

[20] J. Altmeyer, Fundamental characteristics of fricriveted multimaterial joints: effect of process parameters on joint formation and performance, Airbus PhD Day 2012, Madrid, 2012.

[21] S. T. Amancio-Filho, J. F. dos Santos, Entwicklung des Reibnietens als neues Fügeverfahren für Kunststoff und Leichtbaulegierungen, Materialwissenschaft und Werkstofftechnik Nr. 11, 39, 2008, Willey-VCH Verlag GmbH & Co KGaA, Weinhein 2008

[22] D. L. Chung, Composite materials – Science and Applications, 2nd edition, Springer, NY, 2010

[23] CETEX ® PEI data sheet, TenCate Advanced Composites, Netherlands 2011

[24] ASM Materials Handbook Metals, ASM International, USA 2006

[25] G. Pieta Dias, J. F. dos Santos, Friction Spot Welding of a 2198-T8 aluminium alloy: process optimization and parameters, ECAA 2011, 5-7 October 2011, Bremen

[26] ASTM D 5961 M – 08: Standard test method for bearing response of polymer matrix composite laminates, ASTM International, 2010

[27] P. J. Ross, Taguchi techniques for quality engineering, Tata, McGraw- Hill, NY 1988

[28] D. C. Montgomery, Design and analysis of experiments, 5th Edition, NY, John-Willey & Sons Inc 2006

[29] G. Taguchi, S. Chowdhury, Y. Wu, Taguchi's Quality Engineering Handbook, John Wiley & Sons Inc., Hoboken, New Jersey 2005, ISBN 0-471-41334-8

[30] M. J. Donachie Jr., Titanium. A technical guide. 2nd edition, ASM International, Ohio, USA 2010

[31] S. T. Amancio-Filho, J. Roeder, S. P. Nunes, J. F. dos Santos, F. Beckmann, Thermal degradation of polyetherimide joined by friction riveting (FricRiveting). Part I: Influence of rotation speed, Polymer Degradation and Stability 93 (2008), Elsevier Ltd., 2008

[32] ISO 68-1: 1998, ISO general purpose screw threads – Basic profile – Part 1: Metric screw threads, International Organisation for Standardisation

[33] Fiberline Design Manual, Fiberline Composites A/S, Denmark, 2003

[34] 3321-86, Romanian Standard for road bridges, convoys and load classes

[35] Eurocode 3: EN 1993 – 2: 2010, Steel Bridges, European Committee for Standardisation